Performance Analysis of a Solar Assisted Heat Pump System for In-bin Grain Drying

Xinzhuang Gu[1,2], Jianguo Dai[1,2], Haifeng Li[1,2] and Yanjun Dai[1,2]

[1] Institute of Refrigeration and Cryogenics, Shanghai Jiao Tong University, Shanghai (China)

[2] Engineering Research Center of Solar Energy and Refrigeration, MOE (China)

Abstract

A novel solar assisted heat pump (SAHP) system for in-bin grain drying was proposed to solve the problems of poor uniformity and long drying time of grain in depot with higher initial water content in high grain piles. The effects of different operational parameters on the drying performance were numerically and experimentally investigated. The experimental results indicated that the average water content of 3,760 tons of grain dropped from 12.9% to 12.5% after 42 hours of drying. The specific moisture extraction rate of the proposed system and the exergy efficiency of the grain bin were 1.934 kg/kWh and 40.27%, respectively. The operating cost of SAHP grain drying decreased from 5.57 $/t to 1.43 $/t compared with the grain drying machine for the same drying weight. The daily drying capacity increased from 166 t/d to 334 t/d compared with the mechanical ventilation drying for the same water content reduction rate. This investigation provided guidance for expanding future researches on the SAHP system applied for in-bin grain drying.

Keywords: Solar assisted heat pump, In-bin grain drying, Heating capacity, Drying capacity

1. Introduction

China is the largest grain producer in the world, with the national grain production reaching 669.5 billion kilograms in 2020, of which the output of the three main grains, including rice, wheat, and corn, reached 92%, facing the problem of large drying energy consumption (National Bureau of Statistics of China, 2020). Currently, the grain bin mainly uses the grain drying machine and mechanical ventilation drying equipment for grain drying (Hadibi et al., 2021; Migo-Sumagang et al., 2020; Van Hung et al., 2018). Solar thermal integrated with grain drying is applied to mitigate the contradiction between energy consumption and drying time. Moreover, the combination of solar thermal with heat pump for grain drying can contribute to working in a variety of weather conditions (Xu et al., 2021), especially at night and on cloudy days. Therefore, the integration of solar energy with the heat pump is an economical and efficient grain drying method.

However, as shown in the open literature, many researches have carried out on small-scale grain drying (less than 500 tons) based on solar collectors and heat pump. For example, Hasan Ismaeel and Yumrutaş (Hasan Ismaeel and Yumrutaş, 2020) proposed a solar assisted heat pump system for 50 kg/h wheat drying with an underground storage tank to store more solar heat and dry the wheat steadily. The results showed that the COP of the entire system could be up to 4.3. Li et al. (2018) designed a 300 tons of corn drying system combined multistage series heat pump with the heat pipe, reducing the water content of corn from 34% to 14% with an air flow rate of 132,543 m^3/h. Experimental results showed that the drying cost per unit corn decreased by 22.4% compared with coal-fired drying. In summary, large-scale in-bin grain drying is becoming one of the leading researches and application fields of solar assisted heat pump technology.

Nevertheless, the increase in drying capacity would result in a decrease in drying uniformity and drying speed. Besides, the high temperature and high water content of grain would lead to the reduction of whiteness, affecting the quality of grain. Many literatures have conducted experimental and simulated researches on improving drying uniformity, reducing drying time, and maintaining grain quality. In this respect, Ziegler et al. (2021) evaluated the effect of moisture content, temperature, and storage time on the corn quality. It can be found out that keeping the water content and temperature at 14% and 25℃ and storing the corn for 6 months were the recommended

doi:10.18086/swc.2021.22.10 Available at http://proceedings.ises.org

operating conditions for the bioactive properties of the corn. However, most SAHP systems are not convenient to convert from the heating to the dehumidification scenario, resulting in low working efficiency during rainy days. Moreover, exhaustive researches on evaluating the effectiveness of grain drying are still needed. Therefore, it is necessary to further improve the uniformity in the experiment and discuss the drying effectiveness in the simulation under different weather conditions to expand future researches on in-bin grain drying.

A novel SAHP system applied for in-bin grain drying is proposed to solve the difficulties of poor uniformity and long drying time of grain with higher initial water content in high grain piles. This research aims to evaluate the combined performance of the SAHP system under different working scenarios and analyze the effect of operation parameters on grain drying.

2. Description of the SAHP drying system

The SAHP drying system is divided into three subsystems in Fig. 1: (a) the solar collector subsystem uses solar energy to heat the ambient air, (b) the heat pump subsystem consisting of condenser, expansion valve, evaporator, compressor, and blower, and (c) the grain bin subsystem including air supply pipes, air return pipes, and grain stirrer. As shown in Fig. 2, the SAHP system needs some switches with different drying scenarios according to weather conditions during the grain drying period. he SAHP system has four operating scenarios, which are (a) the solar collector working alone at the time of strong solar radiation, (b) the heat pump working alone at night, (c) the solar collector and the heat pump working together at the time of poor solar radiation, and (d) the heat pump dehumidifying on overcast and rainy days, respectively.

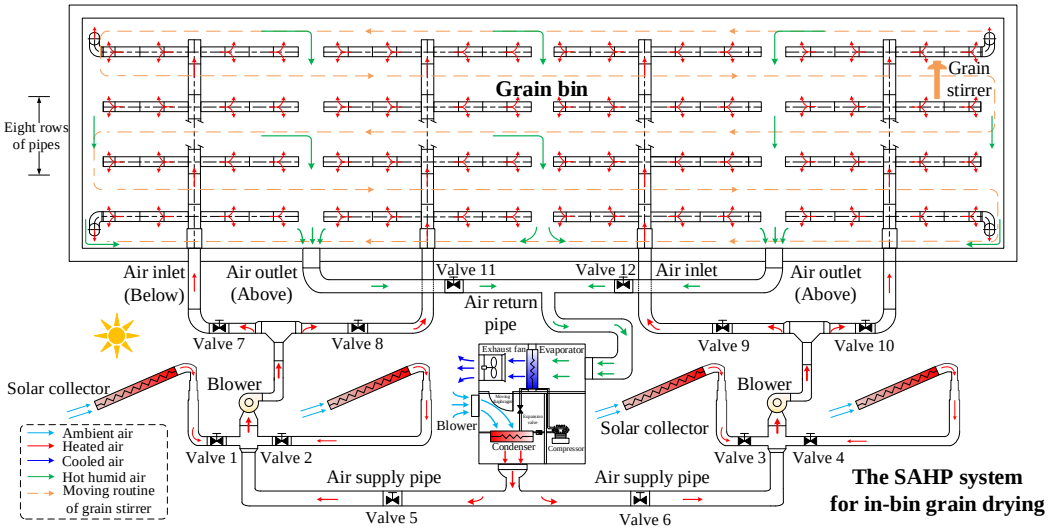

Fig. 1: Schematic diagram of the SAHP system applied for in-bin grain drying

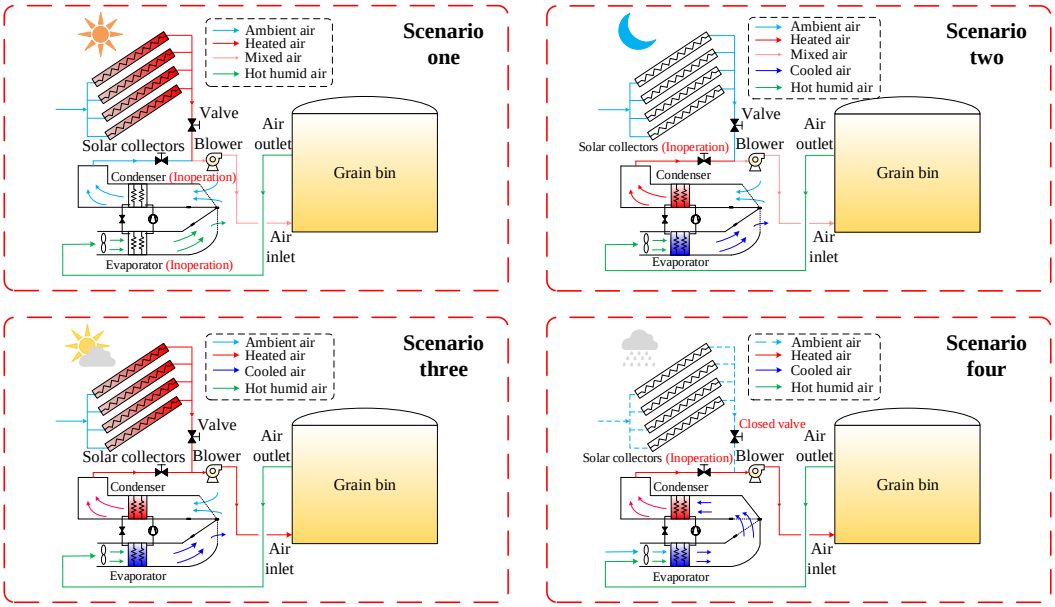

Fig. 2: Four operation scenarios of the entire system under different weather conditions

3. Mathematical model

3.1. Solar collector

The energy equation of the solar collector is (Hawlader and Jahangeer, 2006):

$$M_a c_{p,a} \frac{dT_a}{dt} = A_c \eta_c I_T + m_a c_{p,a} \left(T_{a,out} - T_{a,\text{in}} \right) \quad \text{(eq. 1)}$$

where M_a is the weight of air in the collector, kg; $c_{p,a}$ is the specific heat capacity of air, J/(kg·℃); T_a is the air temperature, ℃; A_c is the collector area, m^2; η_c is the thermal efficiency, %; I_T is the solar radiation intensity, W/m^2; m_a is the mass flow, kg/s; $T_{a,in}$ and $T_{a,out}$ are the temperature of the air at the inlet and outlet respectively, ℃.

The thermal efficiency of the solar collector is calculated by Eq. (2) (Duffie et al., 2020):

$$\eta_c = \frac{\int_{t_1}^{t_2} Q_c dt}{A_c \int_{t_1}^{t_2} I_T dt} \quad \text{(eq. 2)}$$

where Q_c is the effective heat collection of the solar collector, kW.

3.2. Heat pump

The heat transfer of condenser between refrigerant and air is calculated (Iu, 2007):

$$Q_{con} = \varepsilon (mc)_{\min} \left(T_{ht,in} - T_{lt,in} \right) \quad \text{(eq. 3)}$$

where Q_{con} is the heat transfer rate of the condenser, kW; $T_{ht,in}$ and $T_{lt,in}$ are the inlet temperature of high temperature side and low temperature side, ℃.

The input power of the compressor can be calculated as follow (Kong et al., 2017):

$$W_{com,in} = \frac{W_{com}}{\eta_{mo} \times \left(\lambda_T + 0.0025 \times \left(T_{eva} - 273.15 \right) \right)} + \frac{W_m}{\eta_{mo}} \quad \text{(eq. 4)}$$

where η_{mo} is the motor efficiency, %; λ_T is the temperature coefficient; T_{eva} is the evaporation temperature, K; W_m is the friction power, kW.

3.3. In-bin grain drying model

To further describe the variation of grain water content, the modified thin-layer drying model is adopted for this research. The in-bin grain drying model consisted of the following three control equations.

(1) Humidity control equation (Hossain et al., 2003):

$$\Delta H = -\left(\frac{\rho_g}{G_a}\right)\left(\frac{\Delta WC_g}{\Delta t}\right)\Delta z \qquad \text{(eq. 5)}$$

where ΔH is the specific humidity different, kg/kg; ρ_g is the density of grain, kg/m^3; ΔWC_g is the water content different of grain, %; Δt is the time different, s; and Δz is the height different of grain in grain bin, m.

(2) Temperature control equation (Hossain et al., 2003):

$$\Delta T = \frac{\left(\left(c_{p,v} - c_{p,w}\right)T + r_{vap}\right)\times \Delta WC_g}{c_{p,g} + c_{p,w}M_g + \left(c_{p,w} - c_{p,v}\right)\times \Delta WC_g + \frac{G_a}{\rho_g}\times\left(c_{p,a} + c_{p,v}H\right)\times\frac{\Delta t}{\Delta z}} \qquad \text{(eq. 6)}$$

where ΔT is temperature different, ℃; r_{vap} is latent heat of vaporization, kJ/kg; $c_{p,a}$, $c_{p,g}$, $c_{p,v}$ and $c_{p,w}$ are specific heat of air, grain, vapor and water, kJ/(kg·K).

(3) Water content control equation (Dai et al., 2008):

$$\frac{WC_g - WC_e}{WC_0 - WC_e} = \exp\left(-kt^{0.64}\right) \qquad \text{(eq. 7)}$$

where WC_0 and WC_e are initial and equilibrium water content of grain, %.

3.4. Exergy and economic analysis

The exergy flow of air and refrigerant is shown in Eq. (8) and Eq. (9), respectively (Singh et al., 2020a).

$$Ex_a = m_a c_{p,a}((T_a - T_o) - T_o \ln(\frac{T_a}{T_o})) \qquad \text{(eq. 8)}$$

$$Ex_{ref} = m_{ref}((h_{ref} - h_o) - T_o(s_{ref} - s_o)) \qquad \text{(eq. 9)}$$

The payback period of the SAHP system is calculated by Eq. (10):

$$P_p = \frac{C_{ii}}{T_s - C_{ii} - C_{oc}} \qquad \text{(eq. 10)}$$

where C_{ii} and C_{oc} are the initial investments and operating costs of SAHP system, respectively; T_s is the total sales of grain, $.

3.5. Performance evaluation

The specific energy consumption (*SEC*), specific thermal energy consumption (*STEC*), and specific moisture extraction rate (*SMER*) are calculated to evaluate the energy consumption in the drying process (Singh et al., 2020b).

$$SEC = \frac{\int_{t_1}^{t_2}(W_{in,com} + W_{in,bl} + W_{in,gs} + I_T + Q_{con})dt}{M_w} \qquad \text{(eq. 11)}$$

$$STEC = \frac{\int_{t_1}^{t_2}(I_T + Q_{con})dt}{M_w} \qquad \text{(eq. 12)}$$

$$SMER = \frac{M_w}{\int_{t_1}^{t_2}(W_{in,com} + W_{in,bl} + W_{in,gs} + I_T + Q_{con})dt} \qquad \text{(eq. 13)}$$

where M_w is the weight of water removed from grain, kg.

4. Results and discussion

4.1. Performance of SAHP system

As shown in Fig. 3, the combined operation performance of solar collectors and heat pump on a typical sunny day in Kunming was described. The solar radiation was similar to sinusoidal variation, rising from 253 W/m^2 to 1,165 W/m^2 and then dropping to 135 W/m^2. The temperature gradually rose from 7.8℃ to the highest temperature of 16.5℃, then slowly dropped to 15.4℃. The heating capacity of solar collectors was greatly affected by solar radiation, which was also similar to sinusoidal variation, rising from 9.2 kW to 83.5 kW and then dropping to 10.7 kW. The heat produced by the heat pump was less affected by the ambient temperature and the solar radiation, gradually rising from 58.23 kW to the maximum heat produced by 67.39 kW and then slowly falling back to 65.88 kW. Between 11:00 and 16:00, the fraction of solar energy was greater than 0.4, in which it was recommended to turn on the solar collector to obtain better economic performance.

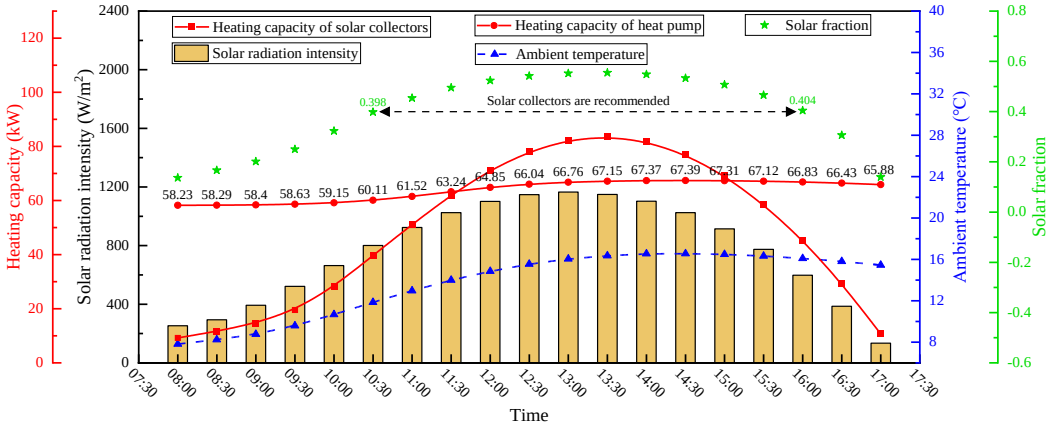

Fig. 3: Simulation of combined operation performance of SAHP system in a typical sunny day

4.2. Simulation of in-bin grain drying

The width, depth, and height of the grain pile model are set to 1 m, 1 m, and 2 m, respectively, and the initial water content of the grain is assumed to be 20%. Fig. 4(a)-(c) show the influence of temperature and relative humidity of inlet air on the grain drying. Take the inlet air temperature at 20℃ and relative humidity at 60% as an example. The initial and final drying stagnation times are 4 h and 8 h, respectively, indicating that the effectual drying time is 12 h, and the water content of grain after drying is 17.56%. Based on the analysis of the inlet air with relative humidity of 60%, when the temperature of the inlet air rises from 20℃ to 30/40℃, the effectual drying time increases from 12 h to 16/18 h, and the water content of grain after drying decreases from 17.56% to 15.76/14.33%. In addition, with the decrease of the relative humidity of the inlet air, the drying effect gets better. For the inlet air with a relative humidity of 30%, the final drying stagnation time decreases to 0 when the temperature rises to 35℃. The inlet air with the relative humidity of 20% has no initial drying stagnation time and final drying stagnation time, indicating that the grain can still be dried by continuing to ventilate.

Fig. 4(d) shows the influence of the wind speed of the inlet air on the drying effect of corn. As the wind speed increases from 0.1 m/s to 0.2/0.3/0.4/0.5 m/s, the drying time decreases from 62 h to 35/26/23/21 h. Fig. 4(e)-(f) describe the effect of wind speed and drying time on the grain drying zone. When the drying time is 10/20/30/40/50 h, the height of the corresponding drying zone is 0.1-0.9 m, 0.3-1.3 m, 0.6-1.6 m, 0.9-2 m, and 1.2-2 m, respectively. For the inlet air with a velocity of 0.5 m/s in Fig. 4(f), it is analyzed that the height of the drying zone corresponding to the drying time of 4/8/12/16 h is 0-2 m, 0.6-2m, 0.98-2 m, and 1.5-2 m respectively.

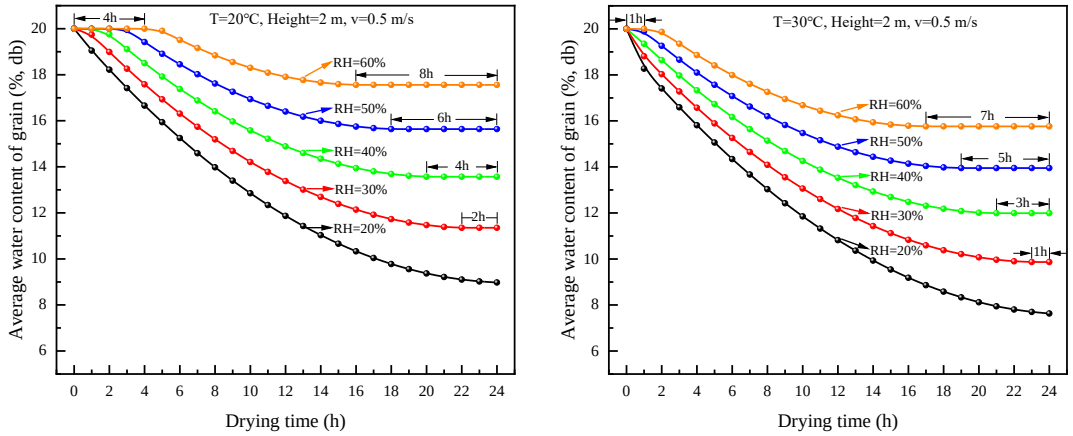

(a) Variation of average water content with different relative humidity at 20°C

(b) Variation of average water content with different relative humidity at 25°C

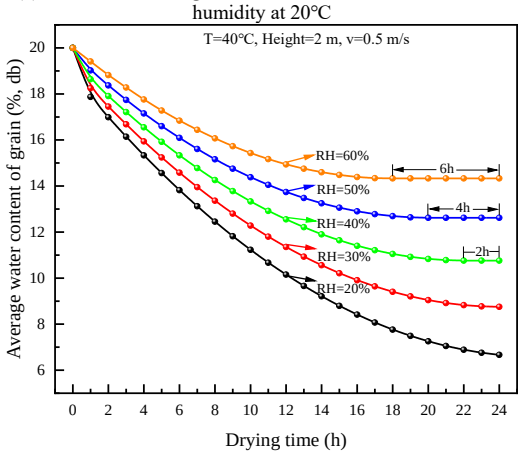

(c) Variation of average water content with different relative humidity at 30°C

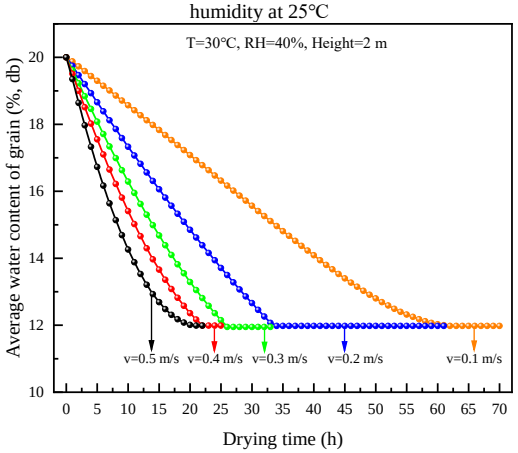

(d) Variation of average water content with different relative humidity at 35°C

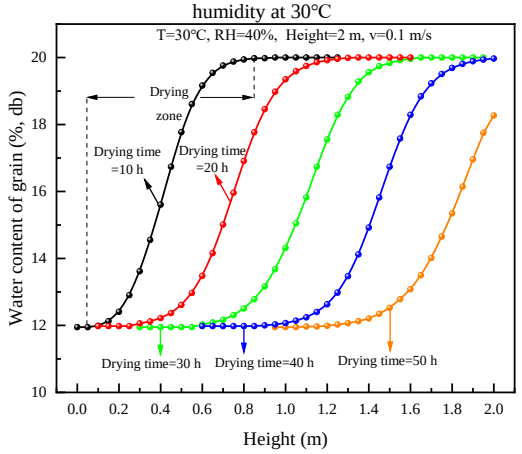

(e) Variation of water content of grain with different drying time

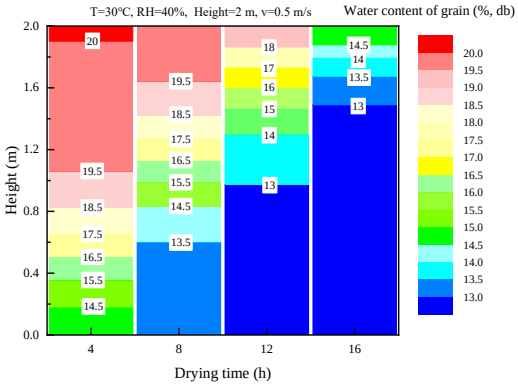

(f) Variation of water content of grain with different drying time and height

Fig. 4: Simulation results of in-bin grain drying

4.3. Drying experiment of SAHP drying system

As shown in Fig. 5, the influence of air parameters at the inlet of the grain bin on grain water content under different weather conditions in summer was tested. The ventilation time on April 30 was from 11:00 to 15:00, during which the solar radiation was relatively good; therefore, ambient air was heated by solar collectors separately. The relative humidity of the air at the inlet of the grain bin varied from 20.8% to 19.4%. The temperature varied from 29.2°C to 36.1°C, which was ranged 4.2-7.5°C higher than the ambient temperature.

On May 1, the solar radiation was relatively good from 9:30 to 14:00, so the ambient air was heated only by solar collectors. The solar radiation was reduced from 14:30 to 16:30. Both solar collectors and heat pump were turned on to prevent the inlet temperature from being too low. The relative humidity of the inlet air varied from 16.9%

to 34.5%, and the temperature varied from 25.2℃ to 38.5℃, which was 3.1-11.85℃ higher than the ambient temperature.

The solar radiation is unstable on May 3. Both solar collectors and heat pump were turned on to heat the ambient air during the day. While the solar radiation intensity was approximately zero after 16:00, the air temperature rose gradually tended to be stable when the system only had the heat pump for heating. The variation of inlet air temperature was from 22.4℃ to 34.7℃, relative to the ambient temperature rise was 7.4-13.8℃, the average temperature rise was 9.3℃, and the relative humidity varied from 14.8% to 32.2%.

For May 4, the ambient air was heated by the combination of solar collectors and heat pump as the solar radiation was poor and unstable between 9:00 to 17:00. Since then, the heat pump was switched to the dehumidification mode for the relatively high humidity of the ambient air, and the temperature rise of the inlet air tended to be stable. The inlet air temperature varied from 22.4℃ to 34.7℃, which is 7.9-14.2℃ higher than the ambient temperature, the average temperature increase was 9.4℃, and the relative humidity variation range was 20.7-37.7%.

The heat pump and solar collectors were turned on May 5 because of the unstable weather. The variation range of air temperature in the grain bin was 26.4-41.8℃, the inlet air temperature rose by 8.5-14.7℃ compared with the ambient temperature, and the relative humidity of inlet air varied in the range of 13.6-36.0%.

The initial value of the average water content of grain was 12.94%, and the average water content of grain after ventilation and drying on April 30, May 1, May 3, May 4, and May 5 was 12.9/12.75/12.61/12.57/12.5%, respectively. Fig. 6 showed the changes in temperature and water content of grain in each layer. The temperature and water content measurement points were located directly above the branch air pipe, in which the first layer was 50 cm away from the branch air pipe, and the spacing of each layer was 100 cm. The temperature of the first layer of grain increased significantly during the ventilation period. The temperature of the first layer was 23.7/24.7/26.3/27.1℃ after ventilation for 0/2/4/6 h, respectively, while the temperature of grain in the area 2 m above the bottom of the grain pile was stable at 20.8℃. The initial values of the average water content of the grain in layers 1-5 were 12.7/12.8/12.7/13.1/13.4%, respectively, the average water content after drying was 12.4/12.7/12.4/12.6/12.7%, respectively, and the water content reduction rate varied from 0.36% to 4.97%.

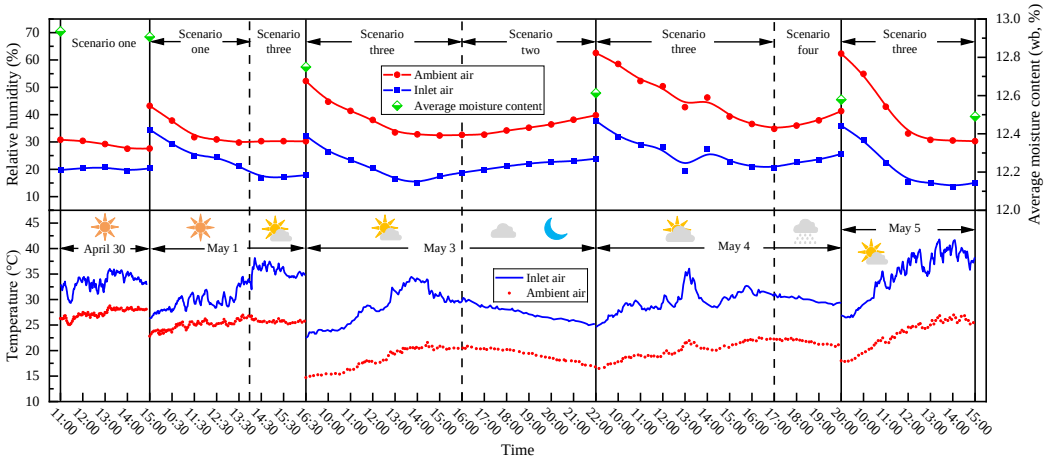

Fig. 5: Experimental results of supply air temperature and relative humidity with different weather conditions in summer

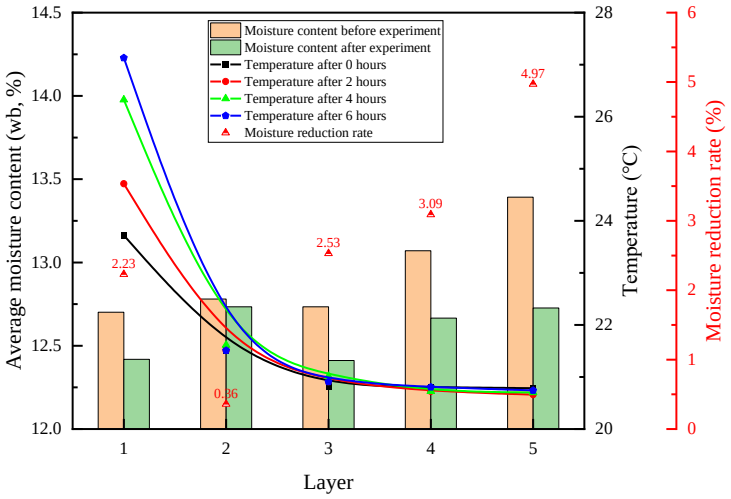

Fig. 6: Experimental results of temperature and average water content changes of grain in different layers

4.4. Energy consumption and exergy evaluation

Fig. 7 depicted the calculation results of *SEC*, *STEC*, and *SMER* under four scenarios. The maximum and minimum values of *SEC*/*STEC* were 3.16/2.7 MJ/kg in scenario one and 1.863/1.48 MJ/kg in scenario three, respectively. The reason was that 11,530 m^3/h and 34,800 m^3/h of ambient air was heated by solar collectors in scenario one and SAHP system in scenario three, respectively, resulting in more water content removed from grain in scenario three than in scenario one. The calculated results of *SEC*/*STEC* in scenario two (2.31/1.78 MJ/kg) are lower than that in scenario four (2.75/2.04 MJ/kg). The reason was that the inlet air flow rate of scenario two (34,800 m^3/h) was larger than that of scenario four (23,270 m^3/h), and RH of inlet air in scenario two (21.6%) was less than that in scenario four (23.1%), resulting in the removal of water content in scenario two was larger than that of scenario four. For the same reason, the maximum and minimum values of *SMER* were 1.934 kg/kWh in scenario three and 1.138 kg/kWh in scenario one, respectively.

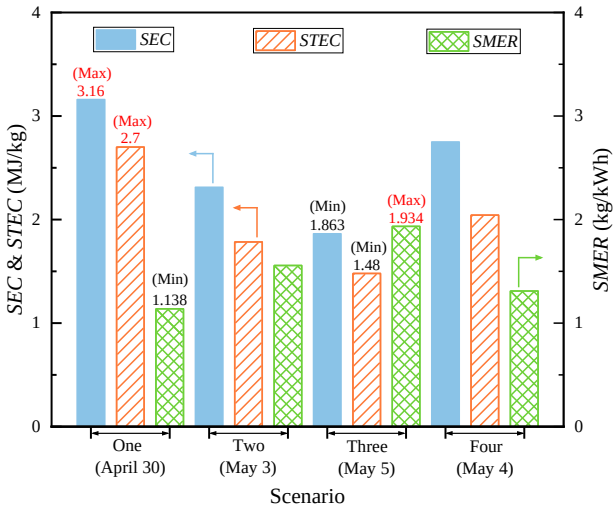

Fig. 7: Calculation results of *SEC STEC* and *SMER* under four scenarios

The exergy flow of inlet and outlet air and exergy destruction of each component of the SAHP grain drying system were described in Fig. 8. The maximum and minimum exergy flow of heated air at the inlet of the grain bin were 14.5 kW in scenario three and 10.84 kW in scenario four, respectively, which was due to the additional air heated by solar collectors in scenario three compared with scenario four. Since the temperature and pressure of the inlet air decreased in the process of grain drying, the exergy destruction and exergy efficiency of the grain bin under four scenarios were 7.9/8.09/8.96/7.31 kW and 39.32%/39.08%/40.27%/35.54%, respectively.

The exergy destruction and exergy efficiency of solar collectors in scenario one and in scenario three were

62.4/46.16 kW and 6.67%/5.26%, respectively. The reason that exergy efficiency of solar collectors was lower than thermal efficiency was that the outlet air temperature was lower than the apparent solar temperature. The exergy destruction and exergy efficiency of the condenser in scenario two, scenario three, and scenario four were 5.1/5.36/4.9 kW and 45.51%/44.16%/46.79%, which was due to higher outlet air temperature in scenario four than that in scenario two and scenario three.

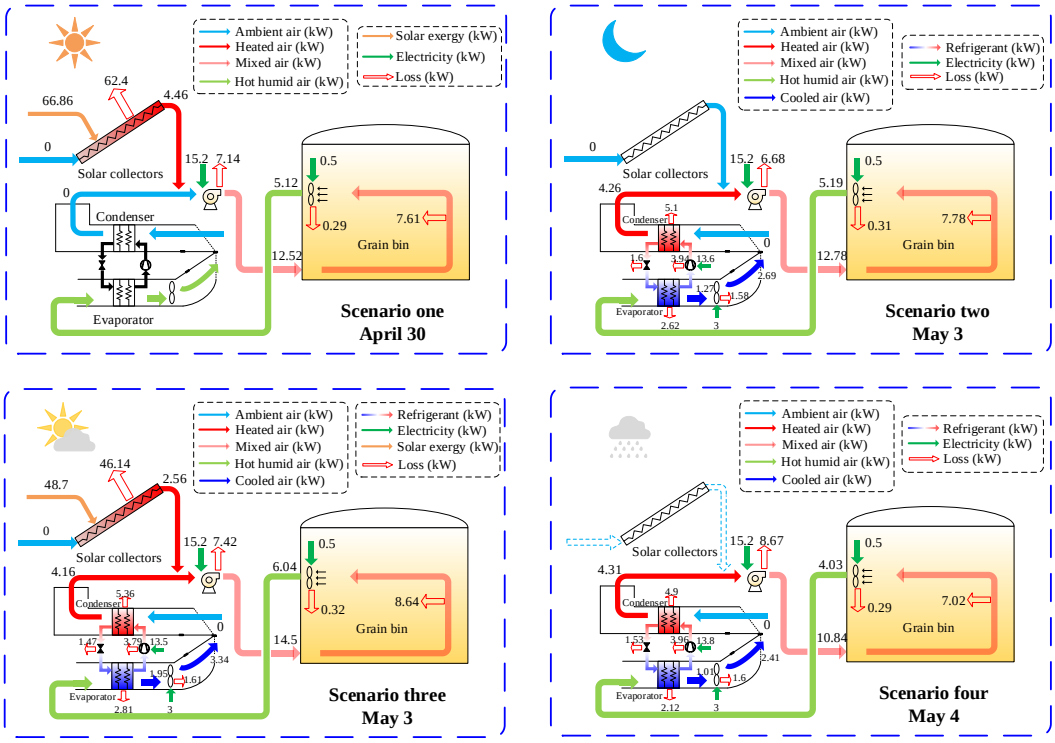

Fig. 8: Exergy analysis of the SAHP grain drying system under four scenarios

4.5. Economic evaluation

Fig. 9 and Table 1 take the mechanical ventilation drying and the grain drying machine as a reference to compare and analyze the economics of the SAHP grain drying. The mechanical ventilation drying generally uses the air supply system to directly send ambient air into the grain bin for drying, whose advantages are the lowest operating cost, initial investment, and payback period, which are 1.06 $/t, 22,930 $, and 0.14 years, respectively. Although up to 5,000 tons of grain can be dried, the air supply temperature of mechanical ventilation is the same as the ambient temperature, resulting in longer drying time, poor drying uniformity, and being affected by ambient air.

The ambient air can be heated to 50℃ by the grain drying machine, which has the advantages of better drying uniformity and flexible operation modes. However, the drawback of the grain drying machine is the highest operating cost, initial investment, and payback period, which are 5.3 times, 2.4 times, and 3.57 times that of mechanical ventilation drying, respectively. The reason for the high operating cost is that the proportion of fuel cost is 65.6%; in addition, the daily drying capacity of the grain drying machine is relatively small.

The average air supply temperature of the SAHP system for in-bin drying is 40℃. The daily drying capacity of grain is 334 tons/d, which is 2 times and 4.3 times of mechanical ventilation drying and grain drying machine. The operating cost, initial investment, and payback period of SAHP grain drying are respectively 1.485 $/t, 45,850 $, and 0.33 years, which are higher than mechanical ventilation drying due to the high maintenance cost of machinery. The SAHP grain drying has the advantages of larger daily drying capacity, better drying uniformity, and higher air supply temperature compared with the mechanical ventilation drying. Moreover, the SAHP grain drying solves the shortcomings of the grain drying machine due to lower operating costs and initial investment, more weight of dryable grain, and larger water content reduction. In summary, the SAHP grain drying is an economical and efficient method to gradually replace mechanical ventilation drying and grain drying machine.

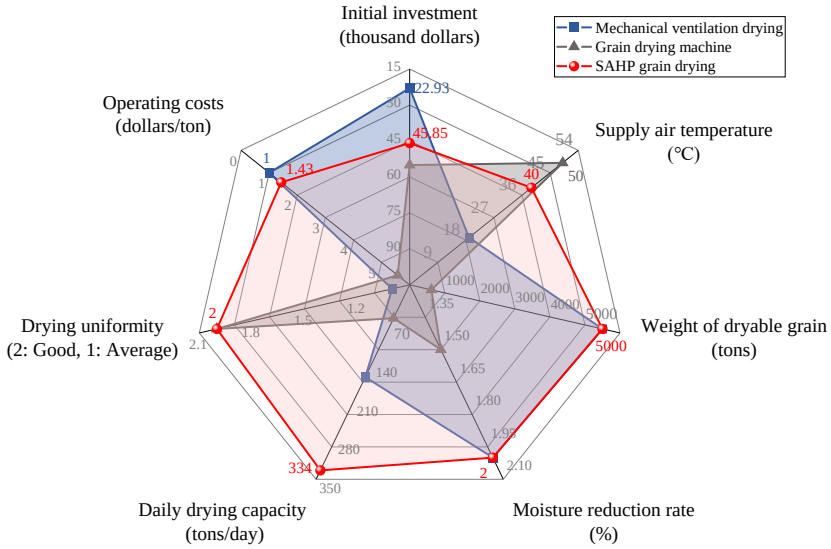

Fig. 9: Economic comparison of three drying technologies

Table 1. Operating costs comparison of three grain drying technologies

Parameters	Mechanical ventilation drying	Grain drying machine	SAHP drying
Maintenance cost ($/t)	0.56	1.53	1.12
Labor cost ($/t)	0.15	0.38	0.08
Electricity cost ($/t)	0.29	0.14	0.23
Fuel cost ($/t)	0	3.52	0
Operating costs ($/t)	1	5.57	1.43

6. Conclusion

For the purpose of evaluating the comprehensive performance of solar collectors and heat pump on grain drying, the experimental and numerical investigations were performed. The main conclusions are summarized as follows:

(1) The *SEC*, *STEC*, and *SMER* of the SAHP grain drying system in scenario three are 1.863 MJ/kg, 1.48 MJ/kg, and 1.934 kg/kWh, respectively.

(2) The exergy destruction and exergy efficiency of solar collectors, condenser, and grain bin in scenario three are 46.14/5.36/8.96 kW and 5.26%/44.16%/40.27%, respectively.

(3) The initial investment of SAHP grain drying is 16.7% lower than that of the grain drying machine for the same drying weight, and the operating cost decreased from 5.64 $/t to 1.485 $/t for the same drying weight. The daily drying capacity increased from 166 t/d to 334 t/d compared with the mechanical ventilation drying for the same water content reduction rate.

(4) The proposed system solves the shortcomings of conventional drying methods due to quickly and uniformly drying the large-scale grain at a lower operating cost.

Acknowledgments

This research was supported by the National Natural Science Foundation of China (No. 51961165110).

References

Dai, J., Wang, X., Dai, Y., Wei, L., 2008. Simulation and analysis of heat pump drying in-store drying. Grain Storage (03), 25-29.

Duffie, J.A., Beckman, W.A., Blair, N., 2020. Solar engineering of thermal processes, photovoltaics and wind. John Wiley & Sons.

Hadibi, T., Boubekri, A., Mennouche, D., Benhamza, A., Abdenouri, N., 2021. 3E analysis and mathematical modelling of garlic drying process in a hybrid solar-electric dryer. Renew Energ 170, 1052-1069.

Hasan Ismaeel, H., Yumrutaş, R., 2020. Investigation of a solar assisted heat pump wheat drying system with underground thermal energy storage tank. Sol Energy 199, 538-551.

Hawlader, M.N.A., Jahangeer, K.A., 2006. Solar heat pump drying and water heating in the tropics. Sol Energy 80(5), 492-499.

Hossain, M.A., Bala, B.K., Satter, M.A., 2003. Simulation of natural air drying of maize in cribs. Simulation Modelling Practice and Theory 11(7-8), 571-583.

Iu, I.S., 2007. Development of air-to-air heat pump simulation program with advanced heat exchanger circuitry algorithm. Oklahoma State University.

Kong, X.Q., Li, Y., Lin, L., Yang, Y.G., 2017. Modeling evaluation of a direct-expansion solar-assisted heat pump water heater using R410A. International Journal of Refrigeration 76, 136-146.

Li, W., Sheng, W., Zhang, Z., Yang, L., Zhang, C., Wei, J., Li, B., 2018. Experiment on performance of corn drying system with combination of heat pipe and multi-stage series heat pump equipment. Transactions of the Chinese Society of Agricultural Engineering 34(4), 278-284.

Migo-Sumagang, M.V.P., Van Hung, N., Detras, M.C.M., Alfafara, C.G., Borines, M.G., Capunitan, J.A., Gummert, M., 2020. Optimization of a downdraft furnace for rice straw-based heat generation. Renew Energ 148, 953-963.

National Bureau of Statistics of China, 2020. Bulletin on the national grain output in 2020. (2020-12-20)[2021-05-01]. http://www.stats.gov.cn/english/PressRelease/202012/t20201211_1808729.html.

Singh, A., Sarkar, J., Rekha Sahoo, R., 2020a. Experimentation on solar-assisted heat pump dryer: Thermodynamic, economic and exergoeconomic assessments. Sol Energy 208, 150-159.

Singh, A., Sarkar, J., Sahoo, R.R., 2020b. Experimental performance analysis of novel indirect-expansion solar-infrared assisted heat pump dryer for agricultural products. Sol Energy 206, 907-917.

Van Hung, N., Quilloy, R., Gummert, M., 2018. Improving energy efficiency and developing an air-cooled grate for the downdraft rice husk furnace. Renew Energ 115, 969-977.

Xu, B., Wang, D., Li, Z., Chen, Z., 2021. Drying and dynamic performance of well-adapted solar assisted heat pump drying system. Renew Energ 164, 1290-1305.

Ziegler, V., Paraginski, R.T., Ferreira, C.D., 2021. Grain storage systems and effects of moisture, temperature and time on grain quality - A review. J Stored Prod Res 91, 101770.